Fusion Engineering and Design 221 (2025) 115378

Contents lists available at ScienceDirect

Fusion Engineering and Design

journal homepage: www.elsevier.com/locate/fusengdes

# Conceptual study of DTT ICRH antenna designs optimizing remote handling strategy

G. Camera [a,b,c,*], A. Cioffi [d], S. Ceccuzzi [d,e], F. Marino [a,c], F.G. Lanzotti [a,b,c], G. Di Gironimo [a,c,d]

[a] Dipartimento di Ingegneria Industriale, Università degli Studi di Napoli Federico II, P.le Tecchio 80, 80125, Napoli, Italy
[b] Università degli Studi di Padova, 35122, Padova, Italy
[c] Consorzio CREATE, Via Claudio 21, 80125, Napoli, Italy
[d] DTT S.C. a r.l., Via Enrico Fermi 45, 00044, Frascati, Italy
[e] ENEA, Via Enrico Fermi 45, 00044, Frascati, Italy

ARTICLE INFO

*Keywords:*
Divertor Tokamak Test
ICRH antenna
Remote Handling
Radio Frequency analyses

ABSTRACT

The Ion Cyclotron Resonance Heating (ICRH) antenna for the Divertor Tokamak Test (DTT) facility is expected to be not only cantilevered, radially movable and fully cooled, but also remote handled: the additional challenge of the Remote Handling (RH) from the inner of the chamber has been posed. The remote assembly and disassembly will be performed through the HYper Redundant MANipulator (HYRMAN) and clearly require the design of the linking interfaces between the remote handled parts and the components placed behind. But the development of in-vessel Radio Frequency (RF) contacts proved in the past to be very challenging, raising concerns on their long-term reliability. Therefore, the toroidal size of the current straps has been reduced to make them, and the relative RF contacts, directly pass through the Vacuum Vessel equatorial port. Thus, only the leftover geometry of the ICRH antenna frontal part should be remote handled and alternative RH strategies have been analyzed and compared. The selecting criteria have been based on the requirements to be fulfilled like the payload limit of the HYRMAN and the RF performance, and on the subcomponents functions to be guaranteed like the side straps shielding. Furthermore, the choice process has also considered technical reasons such as the number of RH operations and interfaces to robotic arms, the minimum number of cooling circuits and the flexion risk. In compliance with the chosen criteria, the most satisfying solution has been selected to be considered for the design of the gripper to be attached to the HYRMAN.

## 1. Introduction

The Divertor Tokamak Test (DTT) facility, which construction is ongoing in Frascati, Rome, will play a key role in the European fusion research roadmap [1] by providing innovative solutions to the heat exhaust problem under ITER and DEMO relevant conditions [2]. These scenarios are reached with a large additional heating power mix and the Ion Cyclotron Resonance Heating (ICRH) antenna package will be able to provide up to 9 MW, in the frequency range of 60–90 MHz, out of the total maximum planned of 45 MW [3,4]. The total amount of the power injected will depend on the number of ports employed by the antennas (see Fig. 1), as a maximum coupled power of 1.5 MW for each antenna has been fixed for DTT [4].

The DTT ICRH antenna system lies on the middle plane region (`port#3`) and its architecture [5] is characterized by a cantilevered structure with an in-chamber frontal part. The VV Port area measures 680 mm in the toroidal dimension and 900 mm in the poloidal dimension. The usable area of the port, shown in red in Fig. 2, is defined as 15 mm from the duct walls and 115 mm from the bottom duct wall due to the presence of the First Wall cooling pipes, thus the usable area is 650 mm toroidal and 770 mm poloidal dimensions. The Antenna dimensions are 1034 mm toroidal and 690 mm poloidal, as illustrated in Fig. 2. As it is toroidally wider than the port to couple the required power, there is the need not only for an active cooling system [6] and the radial movement [5], but also for an in-vessel assembly performed by the Remote Handling (RH).

The DTT RH activities will be carried out by the means of the robotic arm HYper Redundant MANipulator (HYRMAN). It is made of a planar arm and a dextereous arm appropriately designed to guarantee the full reachability of the Vacuum Vessel (VV) inner surfaces of a certain sector entering into the tokamak from the `port#3` [7].

The DTT ICRH antenna frontal part will be remotely handled by the HYRMAN and, as both the robotic arm and the antenna lie in the middle-plane region, the full range of motion of the dexterous part

* Corresponding author at: Dipartimento di Ingegneria Industriale, Università degli Studi di Napoli Federico II, P.le Tecchio 80, 80125, Napoli, Italy.
*E-mail address:* gianluca.camera@unina.it (G. Camera).

https://doi.org/10.1016/j.fusengdes.2025.115378
Received 17 January 2025; Received in revised form 4 July 2025; Accepted 30 July 2025
Available online 13 August 2025

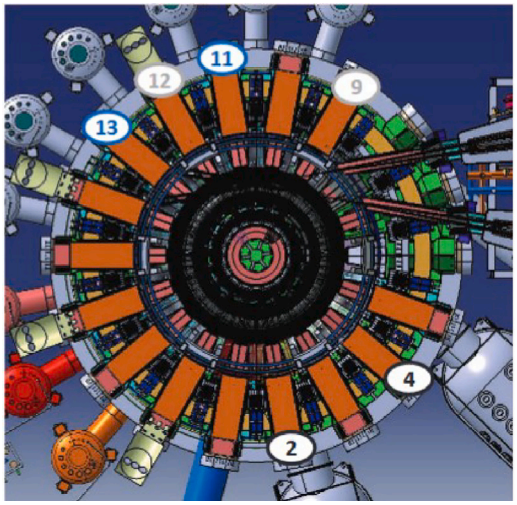


**Fig. 1.** DTT sectors potentially available for ICRH antennas [4].

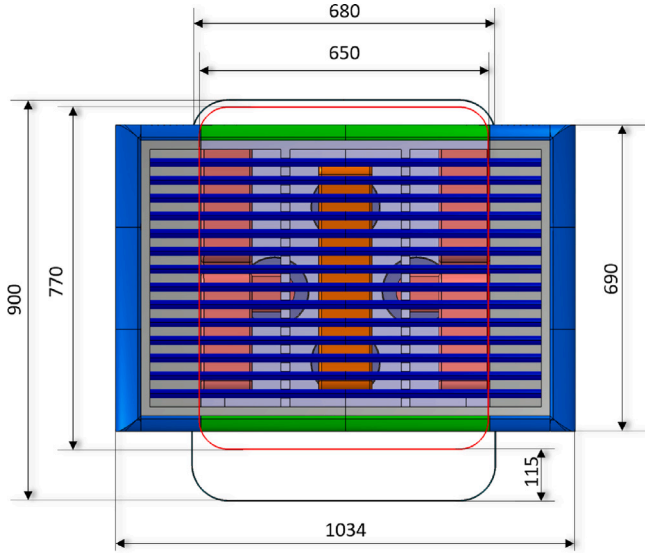


**Fig. 2.** Antenna and Port 3 Dimensions, usable area in red.

is not needed. It can be therefore removed to increase the payload, considering a smaller set of degrees of freedom for safety and precision. The antenna leftover geometry will directly come from the port and therefore linking interfaces between the remote-handled parts and the plug-in ones should be designed, but the in-vessel RF contacts, i.e. among the plug-in coaxial conductors and the remote-handled ones attached to the current straps, have shown few limits especially on the long-term reliability [8]. For this reason, the toroidal extension of the current straps has been reduced to let them and the relative RF connections be plugged in. An alternative RH strategy should be decided to perform the assembly.

Different antenna geometries have been already explored in view of DEMO [9] analyzing the RF performance by varying the number of current straps and the Faraday Screen (FS) architecture. However, as those antennas are wider than the port but they are not cantilevered, a plug-in assembly through either two toroidal arranged halves or two poloidal ones has been proposed. Instead, the present work aims to investigate which antenna geometry split-up better fits the RH requirements and is compliant with the functions to be provided, and to validate and choose the solution through the RF analyses (see Fig. 3).

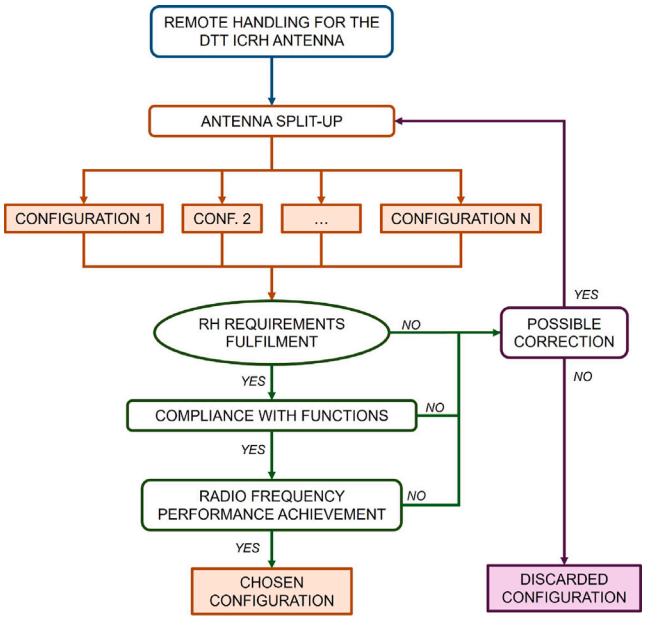


**Fig. 3.** Algorithm for the RH strategy choice.

## 2. Antenna split-up

Several geometrical splits of the antenna frontal part have been considered (see Fig. 4). The options A, B show a traditional continuous FS, while the ones from 1 to 4 want to investigate the possibility to have a partial opened and/or a toroidally separated by septa FS. Indeed, a cantilevered, slotted and internally cooled FS has been studied in Tore Supra [10] showing good thermomechanical properties due to a higher number of degrees of freedom of the bars in spite of RF-sheath effect issues. While a FS toroidally divided by septa has been designed for the second ICRH antenna for EAST [11].

To decide whether a geometrical split-up is suitable for RH purposes, the following RH requirements shall be considered, where "ID" stands for the "IDentifier" used to keep track of the specific RH requirement for the gripper "RH_GRP":

- HYRMAN payload: "The system shall be within the 600 kg at 1000 mm torque limit from the Planar Arm interface". (ID = "RH_GRP.2.2").
- Pipe geometry outside Cut&Weld zone: "The piping system outside the Cut&Weld zone shall allow the passage of all the robotic systems involved in the Cut&Weld operation". (ID = "RH_GRP.1.3.1").
- Pipe geometry in Cut&Weld zone: "The piping system in the Cut&Weld zone shall allow the execution of the operation". (ID = "RH_GRP.1.3.2").

The requirement "HYRMAN payload" [RH_GRP.2.2] defines the maximum torque applicable from the Antenna Box on the Planar arm of the HYRMAN robotic system, thus providing an upper limit on the total mass that shall be remote handled. On the other hand, all Cut&Weld operations are performed in-bore, thus requirement "Pipe geometry outside Cut&Weld zone" [RH_GRP.1.3.1] states the necessity of having at least 60 mm outer diameter pipes to allow the Cut&Weld robot to move inside the pipes, while the requirement "Pipe geometry in Cut&Weld zone" [RH_GRP.1.3.2] states the necessity of providing sufficient clearance around the piping for the execution of the Cut&Weld operations. While precise definition of constraints from the Cut&Weld operations are yet to be fully defined, it is clear that the minimization of independent cooling circuits is vital to the ease of the Remote Handling of the Antenna Box.

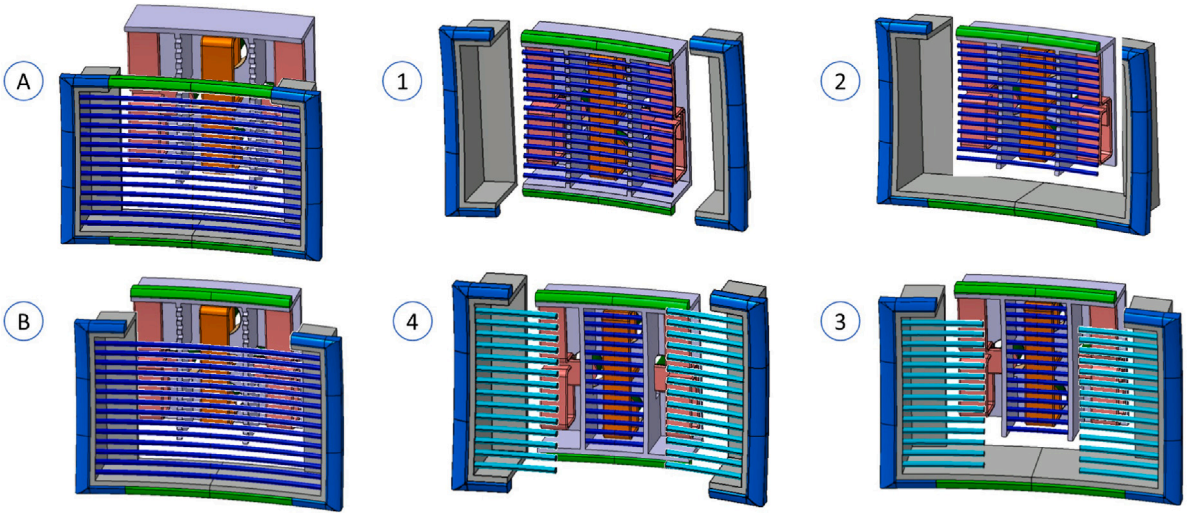


**Fig. 4.** Antenna geometry split-up for remote handling.

These requirements can be respectively translated into the following classification parameters "P. N°":

- Mass of the remote-handled parts (ID = "P.1" from RH_GRP.2.2): the lower it is, the higher the mass of the gripper and the interfaces can be.
- Number of independent cooling circuits for the FS and the frame, "Number of cooling circuits for the FS + number of cooling circuits for the frame" in Table 1 (ID = "P.2" from RH_GRP.1.3.1 and RH_GRP.1.3.2): it should be the lowest possible to ease the RH Cut&Weld operations.

Additional parameters can come from the functions to be guaranteed, and therefore they are adopted in the classification procedure:

- Number of RH operations (ID = "P.3"): the higher it is, the higher the stop time will be. Cut&Weld operations are also counted, "HYRMAN operations + Cut&Weld operations" in Table 1. Important to notice that for a single cooling circuit the Cut&Weld operations are at least 2, considering different operations for inlet and outlet only for Remote Handled parts.
- Interfaces to robotic arms (ID = "P.4"): it depends on the number of interface surfaces for Remote Handling. Indeed, different interfaces are needed on the box to be coupled with the HYRMAN end-effector. Interfaces to Cut&Weld robots are also counted, "HYRMAN interfaces + Cut&Weld interfaces" in Table 1.
- Side straps shielding (ID = "P.5"): it is defined as a percentage relatively to the continuity of FS. For example, if the FS is divided in half, the percentage is defined as 50.
- Flexion risk (ID = "P.6"): a boolean parameter relatively to the front of the Antenna, it is true ($T$) if the Remote Handled component is wider than taller and false ($F$) otherwise.

The comparison among the different proposals is shown in Table 1 where the considered materials for the limiter, the FS and the case are tungsten, Titanium Zirconium Molybdenum (TZM) and Stainless Steel (SS) 316, respectively.

The solution "A" has been pointed out as the most promising candidate. Although its weight is the highest among the different options, it still complies with the requirement RH_GRP.2.2. As the FS and the limiter are not cut, this option provides a complete shielding of the straps and there is the upper part of the limiter linking the two sides of the box. For the same reasons, it especially requires the lowest number of independent cooling circuits for the FS and the frame. Moreover, only a single RH operation is requested for its assembly with three contact interfaces limited to small areas on the bottom, side and top parts of the box.

**Table 1**
Comparison of antenna splits.

| Concept | P.1 [kg] | P.2 | P.3 | P.4 | P.5 [%] | P.6 |
|---|---|---|---|---|---|---|
| A | 270 | 1+1 | 1+2 | 3+2 | 100 | T |
| B | 250 | 1+2 | 1+2 | 3+4 | 100 | T |
| 1 | 83 | 1+4 | 2+4 | 6+6 | 80 | F |
| 2 | 210 | 1+2 | 1+2 | 3+4 | 80 | T |
| 3 | 235 | 3+2 | 1+2 | 3+4 | 90 | T |
| 4 | 94 | 3+4 | 2+4 | 6+6 | 90 | F |

## 3. Radio frequency analyses

Previous split-up solutions have been assessed from an RF point of view with CST Studio Suite to compare them also in terms of RF performance. The reference design of the ICRH antenna of DTT is a three-strap coupler with four coaxial feeds, two of which powering an end-fed, center-grounded, central strap and the other two individually feeding lateral straps. From the RF perspective, considered RH solutions only differ in the FS configuration. Models A–B have traditional FS bars spanning all antenna front and grounded at both septa and box walls. Models 1–2 have FS bars with a clean poloidal cut at the external edge of the lateral straps, making them no longer grounded at the walls of the antenna box. In models 3–4, the FS bars in front of lateral strap housings have a gap of 20 mm from septa walls.

The simulations have been focused on the following design requirements regarding electric field values [4]:

- Absolute value of the electric field, $|E|$, less than 2.5 MV/m everywhere in the antenna box,
- Absolute value of the electric field toroidal component, $|E_{\text{toroidal}}|$, less than 1.5 MV/m everywhere in the antenna box,
- Electric field component parallel to the DTT magnetic field, averaged in front of an antenna side limiter, $\langle E//\rangle$, to be minimized.

The last one is a widely used figure of merit to assess the reduction of RF-induced sputtering [9,12].

Calculations have been run in the worst scenario in terms of electric field values, that is, for a frequency of 90 MHz and a strap phasing equal to $0\pi 0$. $|E|$ and $|E_{\text{toroidal}}|$ have been computed considering all four coaxial transmission lines, feeding the straps, operating at the highest safe value, defined by a standoff voltage of 35 kV.

To better match the plasma shape, the geometry of DTT ICRH antenna presents a double curvature, i.e. over both toroidal and poloidal direction [5], as can be also observed in Fig. 4. Nevertheless, similarly

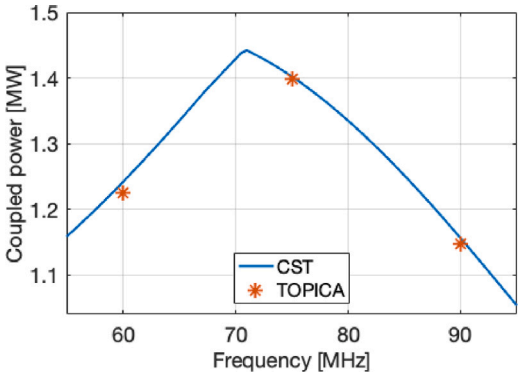


**Fig. 5.** Power coupled by a DTT 3-strap antenna as predicted by TOPICA with an accurate plasma model and by CST Studio Suite with an equivalent homogeneous dielectric load ($\epsilon_r = 225$, $\tan\delta = 1.17$ at 90 MHz) emulating the plasma. The dielectric load is placed at a distance of 60.8 mm from the Faraday screen front.

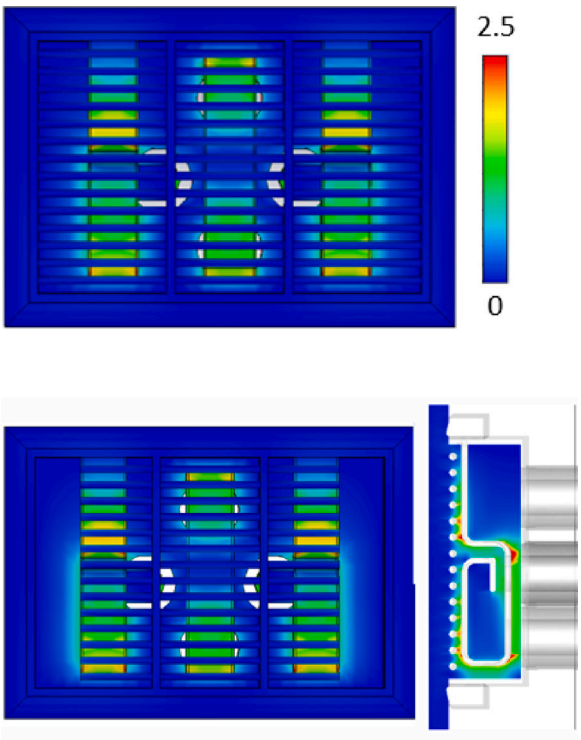


**Fig. 6.** $|E|$ inside models A–B (top) and 1–2 (bottom). Scale values are between 0 and 2.5 MV/m.

to [9], all analyses have been done with dielectric-loaded flat models. The electromagnetic parameters of the dielectric load have been determined by fitting the results of earlier accurate simulations, carried out for a similar, 3-strap, antenna design radiating in front of a DTT reference plasma [4]. More precisely, the coupling performance was used as predicted by TOPICA [13] assuming a clearance of 30 mm between the separatrix and the antenna limiter. The best fit, which can be appreciated in Fig. 5, resulted with a dielectric constant $\epsilon_r = 225$ and a loss tangent $\tan\delta = 1.17$ at 90 MHz. Therefore, a homogeneous dielectric load with such parameters has been modeled in CST Studio Suite to carry out the RF analyses of the present paper.

Fig. 6 shows $|E|$ inside the model, respectively obtained for the designs A–B and 1–2. The highest values are present in the same part of the model, with the model 1–2 presenting the higher one. In either case both electric field values are below the limit. In the third case, as

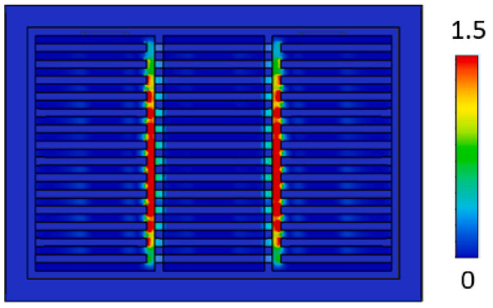


**Fig. 7.** $|E_{\text{toroidal}}|$ inside the model 3–4. Scale values are between 0 and 1.5 MV/m.

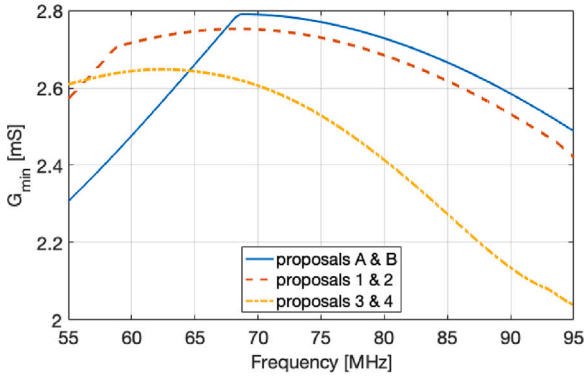


**Fig. 8.** Total antenna minimum conductance across DTT frequency range, calculated with $P_{\text{central}}/P_{\text{outer}} = 1$ and $0\pi0$ phasing.

can be seen in 7, the simulations show that the requirements are not fulfilled.

The third requirement has been taken into account averaging electric field parallel component in a rectangle set at 3 mm in front of the right side limiter. Parametric studies were carried out versus strap phasing and versus the ratio $P_{\text{central}}/P_{\text{outer}}$ of the power coupled by the central strap over the power coupled by the lateral straps, assuming a standoff voltage of 35 kV in the coaxial feed experiencing the highest voltage. The model with the minimum value of $\langle E//\rangle$ for $P_{\text{central}}/P_{\text{outer}} = 1$ and $0\pi0$ phasing is A–B. Models 1–2 and 3–4 resulted instead in very high values of $\langle E//\rangle$.

Fig. 8 depicts the values of the minimum conductance ($G_{\text{min}}$) over the DTT ICRH range of frequencies. $G_{\text{min}}$ is a parameter proportional to the antenna coupling capability and it has been calculated with $P_{\text{central}}/P_{\text{outer}} = 1$ and $0\pi0$ phasing. Owing to the feeding scheme of the ICRH system of DTT [4], the condition $P_{central}/P_{outer} = 1$ indeed corresponds to the preferred working point of the system since it allows for the full exploitation of installed RF power. Proposals A–B and 1–2 are comparable in terms of power coupled all over most part of the frequency range, with models 1–2 exhibiting better performances at low frequencies. The other proposals 3–4, also in terms of coupled power, do not compete with the others.

## 4. Comparison of results and conclusions

Table 2 summarizes the main RF figures of merit at 90 MHz for the considered solutions. Proposals 1–2 and 3–4 have such high field that a further optimization is arguably difficult and with low expectations of tangible improvements with respect to the proposals A–B.

It is worth exploring to some extent the RF capabilities of the most promising options, namely A–B, since analyses conducted so far have been mainly restricted to the working condition with $0\pi0$ strap phasing and $P_{\text{central}}/P_{\text{outer}} = 1$. Fig. 9 shows the dependence of $\langle E//\rangle$ at 90 MHz

**Table 2**
Main RF figures of merit at 90 MHz assuming a $0\pi0$ strap phasing, $P_{central}/P_{outer} = 1$ and a standoff voltage of 35 kV.

| Proposals | $\langle E// \rangle$ [kV/m] | $G_{min}$ [mS] | $\lvert E \rvert$ [MV/m] | $\lvert E_{toroidal} \rvert$ [MV/m] |
|---|---|---|---|---|
| A–B | 0.85 | 2.61 | ≤2.5 | ≤1.5 |
| 1–2 | 3.94 | 2.54 | >2.5 | >1.5 |
| 3–4 | 1.78 | 2.14 | >4.0 | >1.5 |

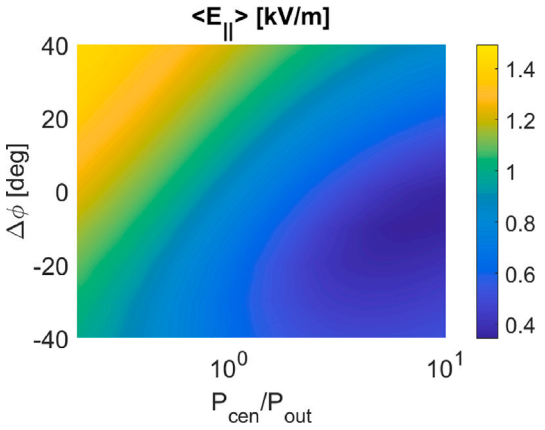


**Fig. 9.** $\langle E// \rangle$ variation sweeping $P_{central}/P_{outer}$ (x-axis) between 0.2 and 10 on a logarithmic scale, and $\Delta\phi$ (y-axis) between −40° and 40°. Plot is obtained at $f$ = 90 MHz and $\langle E// \rangle$ is normalized to fixed coupled power of 1.5 MW.

on the power ratio $P_{central}/P_{outer}$ and on the strap phasing, expressed through the parameter $\Delta\phi$ as a deviation from the condition considered so far (in detail a phasing $0, \pi + \Delta\phi, 0$ is considered). By acting on the feeding signals of the coaxial cable it is possible to move the working point in the deep blue region where $\langle E// \rangle$ takes its minimum values at the cost of shifting the major part of the power on the central strap. Since lateral and central straps are fed with the same number of identical generators, such a change of the working point entails a reduction of coupled power. Similar plots of $\langle E// \rangle$ for proposals 1–2 and 3–4, which are not shown for the sake of brevity, confirm the lower attractiveness of these options since the minimum region is further shifted to higher values of $P_{central}/P_{outer}$, making the change of working point far less convenient than in the options A–B. Anyhow, in those cases moving to the region of minimum $\langle E// \rangle$ would give negligible improvement, because, for any combination of $P_{central}/P_{outer}$ and $\Delta\phi$, the absolute values $\langle E// \rangle$ are too high.

A similar plot to Fig. 9 is reported in Fig. 10, but it shows the $G_{min}$, i.e. the coupling capability of the antenna, as a function of the working point. Looking at Fig. 10 along with Fig. 9 gives a useful point of view on the optimization trade off between raising the coupled power and lowering down parallel electric fields. Moving to the deep blue region in Fig. 9, that is, where the $\langle E// \rangle$ is low on the antenna limiters, involves, in addition to the effects discussed above, a drop in the ability of the antenna to couple power to the load. The current optimization activity of antenna RF design is seeking a superimposition of the deep blue region of Fig. 9 and the light yellow region of Fig. 10, which respectively represent the minimum of parallel E-field component on the side limiters and the highest coupled power. Therefore, from an RF point of view it stands out that solutions A–B must be chosen regardless of the planned working point of DTT antennas.

Hence, the solution "A" has not only been chosen through the comparison in terms of mechanical requirements and functions, but it also provides the better RF performance among the different options. For these reasons, this kind of antenna split-up has been selected for the RH operations and the RH gripper design.

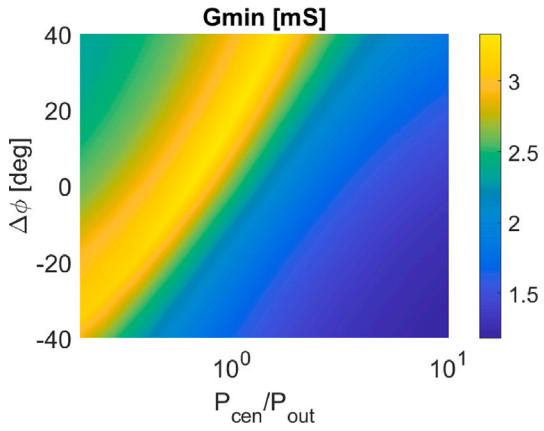


**Fig. 10.** $G_{min}$ variation sweeping $P_{central}/P_{outer}$ (x-axis) between 0.2 and 10 on a logarithmic scale and $\Delta\phi$ (y-axis) between −40° and 40°. Plot is obtained at $f$ = 90 MHz.

## CRediT authorship contribution statement

**G. Camera:** Conceptualization, Visualization, Resources, Investigation, Methodology, Writing - Original Draft, Writing - Review & Editing. **A. Cioffi:** Conceptualization, Formal analysis, Investigation, Writing - Original Draft, Writing - Review & Editing. **S. Ceccuzzi:** Supervision, Formal analysis, Investigation, Resources, Writing - Original Draft, Writing - Review & Editing. **F. Marino:** Methodology, Investigation, Visualization, Writing - Original Draft, Writing - Review & Editing. **F.G. Lanzotti:** Methodology, Writing - Original Draft, Writing Review & Editing. **G. Di Gironimo:** Supervision, Methodology, Resources, Writing Review & Editing.

## Declaration of competing interest

The authors declare that they have no known competing financial interests or personal relationships that could have appeared to influence the work reported in this paper.

## Acknowledgments

The authors would like to thank all the DTT ICRH antenna work package and the CREATE consortium members for their valuable and constant support.

This work has been carried out within the framework of the EUROfusion Consortium, funded by the European Union via the Euratom Research and Training Programme (Grant Agreement No 101052200 - EUROfusion). Views and opinions expressed are however those of the author(s) only and do not necessarily reflect those of the European Union or the European Commission. Neither the European Union nor the European Commission can be held responsible for them.

## Data availability

Data will be made available on request.

## References

[1] T. Donnè, W. Morris, European Research Roadmap to the Realisation of Fusion Energy, Technical Report, EUROfusion, 2018.
[2] F. Romanelli, et al., Divertor Tokamak test facility project: status of design and implementation, Nucl. Fusion 64 (11) (2024) 112015, http://dx.doi.org/10.1088/1741-4326/ad5740.
[3] R. Ambrosino, DTT - divertor Tokamak test facility: A testbed for DEMO, Fusion Eng. Des. 167 (2021) 112330, http://dx.doi.org/10.1016/j.fusengdes.2021.112330.

[4] S. Ceccuzzi, B. Baiocchi, A. Cardinali, G. Di Gironimo, G. Granucci, D. Liuzza, D. Mascali, G.S. Mauro, D. Milanesio, F. Mirizzi, A. Pidatella, S. Piras, C. Ponti, G.L. Ravera, G. Schettini, G. Torrisi, A.A. Tuccillo, G. Vecchi, The ICRF antenna of DTT: Design status and perspectives, in: 24th Topical Conference on Radio-Frequency Power in Plasmas, Annapolis, USA, 2023, 030015, http://dx.doi.org/10.1063/5.0162417.

[5] G. Camera, F.G. Lanzotti, S. Ceccuzzi, G.D. Gironimo, Preliminary conceptual design of the ICRH antenna for DTT: A systems engineering approach, IEEE Trans. Plasma Sci. (2024) 1–7, http://dx.doi.org/10.1109/TPS.2024.3369469, Conference Name: IEEE Transactions on Plasma Science.

[6] R. Marinari, P. Maccari, A.D. Nevo, N. Badodi, S. Ceccuzzi, G. Camera, G. Di Gironimo, Thermal hydraulic and mechanical assessment of the DTT ICRH antenna, in: 20th International Topical Meeting on Nuclear Reactor Thermal Hydraulics (NURETH-20), Washington, DC, USA, 2023.

[7] S. Buonocore, G. Di Gironimo, M. Favaretto, T. Grasso, F. Zanon, S. Grazioso, Systems engineering approach for the iterative concept design and virtual simulation of the DTT hyper redundant manipulator, Fusion Eng. Des. 190 (2023) 113534, http://dx.doi.org/10.1016/j.fusengdes.2023.113534.

[8] J. Hillairet, Z. Chen, G. Lombard, J. Delaplanche, K. Vulliez, Q. Yang, B. Beaumont, F. Calarco, N. Charabot, F. Kazarian, P. Lamalle, J. Bernard, V. Bruno, J. Hatchressian, R. Laloo, P. Mollard, Y. Song, V. Turq, R. Volpe, Radiofrequency and mechanical tests of silver coated CuCrZr contacts for the ITER ion cyclotron antenna, Fusion Eng. Des. 129 (2018) 29–39.

[9] V. Bobkov, M. Usoltceva, H. Faugel, A. Kostic, R. Maggiora, D. Milanesio, V. Maquet, R. Ochoukov, W. Tierens, F. Zeus, W. Zhang, Development of pre-conceptual ITER-type ICRF antenna design for DEMO, Nucl. Fusion 61 (4) (2021) 046039, http://dx.doi.org/10.1088/1741-4326/abe7d0.

[10] Y. Corre, M. Firdaouss, L. Colas, A. Argouarch, D. Guilhem, J. Gunn, C. Hamlyn-Harris, J. Jacquot, M. Kubic, X. Litaudon, M. Missirlian, M. Richou, G. Ritz, D. Serret, K. Vulliez, Characterization of heat flux generated by ICRH heating with cantilevered bars and a slotted box faraday screen, Nucl. Fusion 52 (10) (2012) 103010, http://dx.doi.org/10.1088/0029-5515/52/10/103010, Publisher: IOP Publishing and International Atomic Energy Agency.

[11] X.Q. Yang, Y.T. Song, S.T. Wu, Y.P. Zhao, J.X. Zhang, Z.W. Wang, Mechanical design of the second ICRF antenna for EAST, Fusion Eng. Des. 87 (7) (2012) 1249–1252, http://dx.doi.org/10.1016/j.fusengdes.2012.02.123.

[12] V. Bobkov, D.E. Trindade de Aguiam, R. Bilato, S. Brezinsek, L. Colas, H. Faugel, H. Fuenfgelder, A. Herrmann, J. Jacquot, A. Kallenbach, D. Milanesio, R. Maggiora, R. Neu, J.-M. Noterdaeme, R. Ochoukov, S. Potzel, T. Puetterich, A. Silva, W. Tierens, A. Tuccilo, O. Tudisco, Y. Wang, Q. Yang, W. Zhang, Making ICRF power compatible with a high-Z wall in the ASDEX Upgrade, Plasma Phys. Control. Fusion 59 (1) (2017) 11, http://dx.doi.org/10.1088/0741-3335/59/1/014022.

[13] V. Lancellotti, D. Milanesio, R. Maggiora, G. Vecchi, V. Kyrytsya, TOPICA: an accurate and efficient numerical tool for analysis and design of ICRF antennas, Nucl. Fusion 46 (7) (2006) S476–S499, http://dx.doi.org/10.1088/0029-5515/46/7/s10.